fibers

Article

Quality of Plywood Bonded with Nanolignin-Enriched Cardanol-Formaldehyde Adhesive

Maria Rita Ramos Magalhães [1], Felipe Gomes Batista [1], Ana Carolina Corrêa Furtini [1], Mário Vanoli Scatolino [2,*], Flávia Maria Silva Brito [3], Lourival Marin Mendes [1], Thiago de Paula Protásio [1] and José Benedito Guimarães Junior [1]

[1] Department of Forest Science, Federal University of Lavras (UFLA), Lavras 37200-000, MG, Brazil; mariaritamagalhaes37@gmail.com (M.R.R.M.); felipejp.gomes@gmail.com (F.G.B.); carol.furtini1@gmail.com (A.C.C.F.); lourival@ufla.br (L.M.M.); thiagoprotasio@ufla.br (T.d.P.P.); jose.guimaraes@ufla.br (J.B.G.J.)

[2] Collegiate of Forest Engineering, State University of Amapá (UEAP), Macapá 68900-070, AP, Brazil

[3] Department of Forest Sciences, Luiz de Queiroz College of Agriculture, University of São Paulo (USP), Piracicaba 13418-900, SP, Brazil; faengflorestal@gmail.com

* Correspondence: marioscatolino@gmail.com

Abstract

Cardanol is a derivative of cashew nut shell liquid (CNSL) and has the potential to be used when developing adhesives for wood boards. Adding nanostructures to adhesive can increase its bonding and reduce formaldehyde emission. Therefore, this study aimed to evaluate the different concentrations of nanolignin (1, 2, and 3%) added to the cardanol-formaldehyde adhesive for gluing plywood, in comparison to the cardanol-formaldehyde adhesive without nanolignin (0%). The plywood's physical, mechanical, and formaldehyde emission properties were assessed. Plywoods with nanolignin showed shear strength increases of around 160% in the wet condition. With the addition of nanolignin, the modulus of rupture and of elasticity increased by approximately 150% and up to 400% in the parallel direction, respectively. The resistance to combustion also significantly improved. Physical properties did not show statistically significant differences with the percentages of nanolignin. Despite the increase in formaldehyde emission with nanolignin, all treatments met the marketing requirements ($\leq$80 mg of formaldehyde/kg), demonstrating the adhesive potential for indoor use in plywood industries. Natural adhesives using cardanol and nanolignin are an innovative and ecological alternative, combining sustainability and high potential to reduce environmental impacts, which is aligned with at least four sustainable development goals (SDGs).

Keywords: wood boards; nanotechnology; free formaldehyde; natural adhesives

1. Introduction

Wood can be processed into different shapes and sizes and reconstituted to create new products. To meet this objective, different adhesives and appropriate methods and processes must be used for each product type, application, and end-use. Most adhesives used in wood composites are formaldehyde-based, including phenol-formaldehyde (PF), urea-formaldehyde (UF), and melamine-formaldehyde (MF), due to their excellent adhesion properties [1]. Among polymeric adhesives, PF has been widely used to manufacture wood composites, such as plywood, fiberboard, and particleboard [2,3].

However, these adhesives have the disadvantage of undesirable effects, including respiratory diseases and degradation of air quality, mainly due to free formaldehyde emission [4]. Furthermore, exposure to formaldehyde through regular contact in indoor environments negatively impacts human health, and formaldehyde is classified as a carcinogen by the World Health Organization (WHO) and the US Environmental Protection Agency (EPA) [5,6].

Thus, formaldehyde emission, depletion of petroleum resources, and increasing attention to environmental protection have increased the demand for adhesives made from renewable biological resources [1,7]. In this context, cardanol, a renewable and harmless organic byproduct of the cashew industry, is obtained from agricultural residues removed from cashew nut shells by a commercially viable distillation method [8]. Compared to similar phenolic derivatives, cardanol has a rigid benzene ring and a long, flexible, hydrophobic alkyl chain with multiple unsaturated bonds. Its low volatility and viscosity make it a suitable choice for preparing reactive diluents for petroleum-based epoxy resin [9]. In addition to its structural benefits and renewable nature, its low cost and toxicity make it an attractive candidate over petroleum products [10].

Cardanol also stands out for having high electrical insulation and good thermal stability. Its structure has broad functionality with three reactive sites, phenolic hydroxyl, aromatic ring, and unsaturation in the alzimyl side chain [11]. In addition, it can be polymerized in several ways, with the most common being the production of alkyd adhesives through side chain addition polymerization and the production of phenolic adhesives through condensation polymerization with aldehydes [12,13]. In polymerization with formaldehyde, cardanol presents greater reactivity due to the presence of two hydroxyl groups in the aromatic ring favoring the selective polymerization of CNSL phenolic monomers [14].

Several technological applications have used cardanol, such as in thermosetting matrices in composites reinforced with buriti fibers [15], sugarcane bagasse [16,17], densified laminated wood [18], bio-based polymers and additives [19], and adhesives for particle panels [14,20].

Lignin has also emerged as an advantageous material for developing inexpensive, biodegradable, and environmentally friendly products [21]. The phenolic nature and the presence of several functional groups (OH, COOH, OCH_3, and C=O) in lignin raise the possibility of its value in several fields, such as wood adhesives [22]. In biomass, lignin acts as a natural glue that holds the cellulose fibers within the plant structure, giving it rigidity and strength while also providing water transport and protecting the plant from environmental degradation [2]. Given the high structural similarity of lignin to phenols, lignin is an ideal biological polyphenol to displace phenols in PF matrices and cross-link formaldehyde from the free aromatic C3 and C5 positions, present mainly in the hydroxyphenyl and guaiacyl units [23].

The presence of aromatic ring and robust molecular interactions makes lignin a promising bio-based candidate for reinforcement in polymeric materials [24].

Based on the polyphenol structure of lignin, lignin can be integrated into the polymerization of phenolic adhesive as an alternative to petroleum-derived monomer [25,26]. Most research focuses on the development of thermosetting incorporated phenolic adhesives, which are prepared under alkaline catalysis with formaldehyde/phenol and are generally used as adhesives or foaming precursors. Thermoplastic phenolic resin (novolak resin) is another type of adhesive used in powder, fiber and adhesive molding applications, but lignin-novolak resin attracts less research interest [27–29]. This type of adhesive is prepared under acid catalysis with F/P and thus forms a basically linear molecular structure. As expected, lignin is less reactive than phenol as it has fewer reactive sites available to react

with formaldehyde, limiting the amount of lignin that can be incorporated to achieve the desired curing and mechanical properties [30].

That way, the direct use of Kraft lignin in commercial adhesives, such as PF, requires high pressing time and temperature due to its low reactivity, which can harm the strength of the panels, as in the work of Luckman et al. [31], which showed that the gradual percentage addition of lignins to UF impaired the dimensional stability and strength and stiffness properties of the panels. Therefore, using lignin without modification is not commercially advantageous for this application. Thus, a new approach is seen in obtaining lignin nanostructures since they have a high surface area. When mixed with polymers, they interact closely with the polymer matrix. They can significantly increase the final composite's physical–mechanical performance, thermal stability, and barrier properties compared to lignin without nanoparticularization [32].

Compared to lignin, lignin nanoparticles offer advantages such as regular geometry, controllable size, larger specific surface area, improved dispersion, enhanced compatibility, and better reducibility to metal ions [33]. In addition to chemical interactions, lignin physically incorporated into the adhesive matrix in nanometric form promotes increased structural rigidity, due to its high surface area and dense aromatic nature. Studies such as those by Gong et al. [34] and Liu et al. [30] demonstrate the viability of these interactions and their positive impact on adhesive performance.

Some studies have already demonstrated the use of nanolignin in adhesive formulations. Younesi-Kordkheili et al. [35] developed a cold plywood adhesive based on polyvinyl alcohol (PVOH), maleated nanolignin, and hexamine. Zhu et al. [36] used alkali amine-amplified lignin nanoparticles in wood adhesive.

Considering the above and highlighting the importance of studies on the use of natural products in adhesive formulations, this study aims to analyze the influence of three different concentrations of nanolignin in cardanol-formaldehyde-based adhesives on the physical–mechanical characteristics of boards, as well as intending to reduce formaldehyde emissions. The dynamics of natural adhesives with cardanol and nanolignin are aligned with at least four Sustainable Development Goals (SDGs), including SDG 9—Industry, Innovation and Infrastructure, SDG 12—Responsible Consumption and Production, SDG 13—Climate Action and SDG 15—Life on Land.

2. Materials and Methods

2.1. Preparation of Materials

The species used for plywood production was *Pinus oocarpa*, 18 years old, collected in an experimental plantation located in Lavras, a southern region of Minas Gerais (Brazil), coordinates 21°14′45″ S, 44°59′59″ W and altitude of 920 m. Three trees were cut with a chainsaw and a disc was removed at 1.30 m from the ground for chemical characterization and basic density.

The trees were sectioned into 58 cm logs and heated at 70 °C for 24 h in water to facilitate the lamination. After heating, 2 mm veneers were obtained using a rotary lathe and dried at approximately 105 ± 2 °C for 24 h until reaching 3% (dry basis). Cardanol was supplied by Resibras Cashol, located in Fortaleza (Brazil). The material is liquid and dark brown in color. Kraft lignin was obtained (powder) from *Eucalyptus* sp. from a pulp and paper company. Using a top-down approach, a solution of 300 g of lignin in 3 L of water was prepared and homogenized for 40 min at 500 rpm with a High Torque Mechanical Agitator—NT 134, with adaptations described in Lopes et al. [37]. The lignin nanostructures were obtained by a mechanical process using a Super Masscolloider Masuko Sangyo MKCA6-2 mill with 10 passes at 1500 rpm. The distance between the mill discs was set at 120 μm. The total energy consumption of the process was 4366.39 kWh/t.

2.2. Characterization of the Wood

The basic density of *Pinus oocarpa* was determined following the guidelines of the standard NBR 11941 [38]. The chemical constituents were determined after grinding the raw material in a knife mill, using the fraction that passed through the 40 mesh (0.420 mm), retained in the 60 mesh (0.250 mm) according to the following standards: total extractive content [39]; insoluble lignin content [40]; ash content [41]; and holocellulose content (cellulose + hemicelluloses) obtained according to [42].

Fourier transform infrared spectroscopy (FTIR) was carried out on a Shimadzu IRAffinity-1 spectrophotometer, with samples dried at 60 °C for 3 h. Pellets containing KBr and 5% (w/w) of the sample powder were prepared. For the reference spectrum, a pellet of pure KBr was analyzed. Each spectrum was recorded with 32 scans, using a resolution of 4 cm^{-1}, in the spectral range from 4000 to 400 cm^{-1}.

*2.3. Adhesive Formulation and Characterization*

The cardanol-formaldehyde adhesive was synthesized according to the study by Faria et al. [14]. Paraformaldehyde with a pH of 8.5 and a solid content of approximately 95% to 99% was used. The pH of cardanol was 7.94, with a solid content of 96.91%. Cardanol was heated in a water bath at 90 °C and formaldehyde was added in a ratio of 1:5 (200 g formaldehyde: 40 g cardanol). After 60 min, the catalyst (4.62 g) of NaOH (2.0 M) was added. Once the endpoint was reached, at which the adhesive reaches the desired viscosity, the nanolignin was gradually incorporated into the adhesive, under vigorous stirring with a ballerina, to ensure the homogenization. The application of lignin nanostructures in the adhesive was carried out according to Lopes et al. [37]. The authors applied the mixture of lignin nanoparticle suspension to the adhesive at room temperature at concentrations of 1, 2 and 3%, by mass, based on the total mass of the adhesive.

The adhesives were characterized according to the following properties: solids content ASTM D 1490-01 [43], viscosity ASTM D1200-10 [44] and pH, determined by direct readings on a Tecnal Tec-3mp pH meter. Three samples were evaluated for all tests. The resistance of the adhesive to thermal degradation was evaluated by thermogravimetric analysis (TG), using the Shimadzu DTG-60AH equipment. For each test, 2 mg samples were used, subjected to a heating rate of 25 °C/min, from 30 °C to 600 °C, under a continuous nitrogen flow of 50 mL/min. The curves obtained were analyzed using the software Origin Pro version 8.5.

2.4. Adhesion Performance

Five-layer plywood with dimensions of 300 × 300 × 15 mm was produced. The cardanol-formaldehyde adhesive formulations modified with lignin nanostructures were applied to the wood veneers with a spatula (Figure 1), with a grammage of 280 g/m^2, with pressing cycle parameters of 1.0 MPa, for 10 min at 160 °C using an automatic hydraulic press. After pressing, the boards were acclimatized at 20 ± 2 °C and relative humidity of 65 ± 5%, stored until constant mass. Four types of plywood were produced with different levels of nanolignin (0, 1, 2, and 3%). For each composition, three replicates were produced, totaling 12 plywoods.

To assess the physical and mechanical properties, the panels were subjected to the sawing process to remove the edges, and subsequently to a circular saw to obtain the samples. Table 1 indicates the tests performed and the established standards.
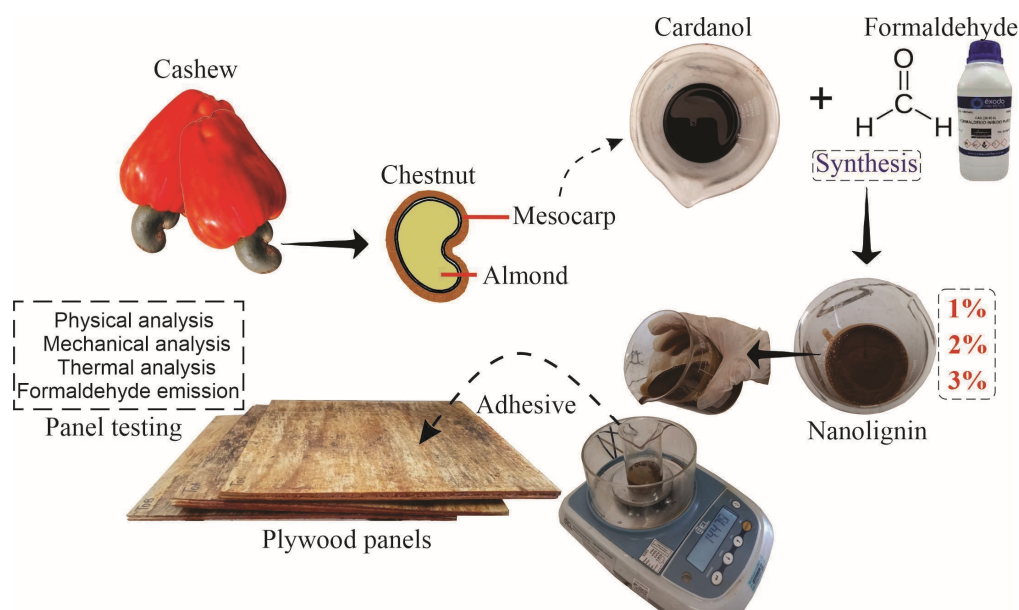
Figure 1. Production of plywood.

Table 1. Physical and mechanical properties of the plywood.

Property	Total Samples	Dimensions (cm)	Standard
Apparent density (g/cm^3)	6	8 × 2.5	NBR 9485 [45]
Moisture (dry basis) (%)	6	8 × 2.5	NBR 9484 [46]
Total water absorption (%)	6	8 × 2.5	NBR 9486 [47]
Shear strength (dry, wet and post-boil) (MPa)	9	10 × 2.5	NBR 12466-1 [48]
Static bending with evaluation of modulus of elasticity (MOE) and modulus of rupture (MOR) (MPa)	9	25 × 5	NBR 9533 [49]

2.5. Microstructural Analysis

After the static bending test, micrographs of the fractured surface regions of the plywood were obtained. The images were acquired using a Zeiss EVO 40 scanning electron microscope (SEM), operating at 15 kV and a probe current of 2 nA. The samples analyzed were previously metallized with gold to ensure electrical conductivity. The micrographs were captured using secondary electron and backscattered electron detectors, with a working distance of 8.5 mm and no sample tilt.

2.6. Formaldehyde Emission

The plywood's free formaldehyde emission was analyzed using the (static) flask method according to European standard 717-3 [50]. The panel samples were suspended in a special device with over 50 mL of distilled water in polyethylene bottles (500 mL). The fully sealed bottles were oven-dried for 3 h at 40 °C. They were then placed at room temperature to achieve complete formaldehyde absorption. Quantification was performed by UV/VIS spectroscopy at 412 nm using the acetylacetone method.

2.7. Thermal Evaluation of Plywood

Thermal evaluation of the boards was performed using the methodology of Setter et al. [51], and Faria et al. [52]. Four samples (2.5 × 2.5 cm) were sectioned per board. The method consists of a device composed of a combustor made of galvanized iron sheet, an aluminum and wood base, a temperature controller, a scale with a precision of 5 mg, and

an aluminum screen that surrounds the combustor to protect it from wind interference during combustion. Mass loss and temperature data were recorded every minute during the test and processed to construct mass × time and temperature × time curves.

2.8. Experimental Design and Data Statistical Analysis

A completely randomized design was adopted to evaluate the treatments with cardanol-formaldehyde adhesives with lignin nanostructures of 1, 2 and 3% for all tests and compared with samples without lignin addition (0%). Analysis of Variance (ANOVA) and Scott–Knott test at 5% significance were performed for all tests.

3. Results and Discussion

3.1. Characterization of Materials

The average basic density of *Pinus oocarpa* was 0.52 g/cm^3 (Figure 2). The basic density may vary according to age and environmental factors. The value found in the study was similar to that observed by Matos et al. [53], who reported a value of 0.53 g/cm^3. Brito et al. [54] found a value of 0.55 g/cm^3 for the same material in their study. The great acceptance of the *Pinus* species is due, in particular, to their medium to low density. However, the chemical composition, anatomical structure, and adhesive content must be considered. According to Iwakiri et al. [55], greater adhesive penetration occurs in low-density woods due to their greater porosity. The adhesive viscosity must be increased to avoid the formation of the "hungry glue line". On the other hand, high-density wood can result in more remarkable dimensional changes, causing greater tension in the glue line.
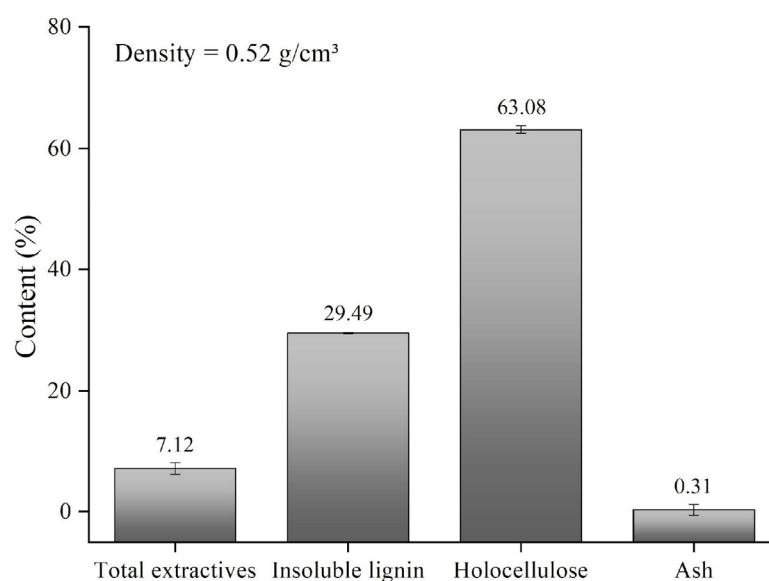
**Figure 2.** Chemical composition and basic density of *Pinus oocarpa*.

In the chemical analyses, the average content of total extractives obtained for *Pinus oocarpa* was 7.12 ± 0.98%, a value close to that reported by Lourenço et al. [56] and Furtini et al. [57], who obtained 6.80% and 7.38%, respectively. According to Santiago et al. [58], the extractive content is one of the most critical parameters for bonding. When found at high levels, it can negatively contribute to the adhesive's curing and polymerization, reducing the board's quality and final performance. Thus, the value found in the present study is acceptable for plywood production.

A value of 29.49 ± 0.13% was obtained for insoluble lignin, relatively similar to those found by Brito et al. [54] at 29.34% and Furtini et al. [20] at 29.20% for the same species. Higher lignin contents in lignocellulosic materials are desirable for reconstituted wood

materials. Despite being considered a natural adhesive, lignin can provide a higher quality of panel adhesion [2]. Due to its aromatic structure, lignin is more hydrophobic than the holocellulose fraction. The average holocellulose value was 63.32%, similar to that obtained by Villarruel et al. [59] (63.29%). Holocellulose has hydroxyl groups that increase the capacity of the wood concerning water adsorption [60].

The value for the ash content obtained in this study was $0.31 \pm 0.09\%$. This property is directly related to the varieties of the material, type of fertilization, cultivation conditions, growth site, age, and several other factors [54]. The presence of high ash concentration can block the reactive sites for adhesion with polar adhesives, affecting the bonding quality and mechanical performance [61]. Thus, the chemical composition of *Pinus oocarpa* wood shows that this material does not limit the production and veneer quality.

In Figure 3, transmittance curves by wavenumber resulting from the FTIR analyses are plotted. It was possible to observe similar chemical bonds present in the cardanol and the cardanol-formaldehyde adhesive, represented by different transmittance intensities (Figure 3a,b).
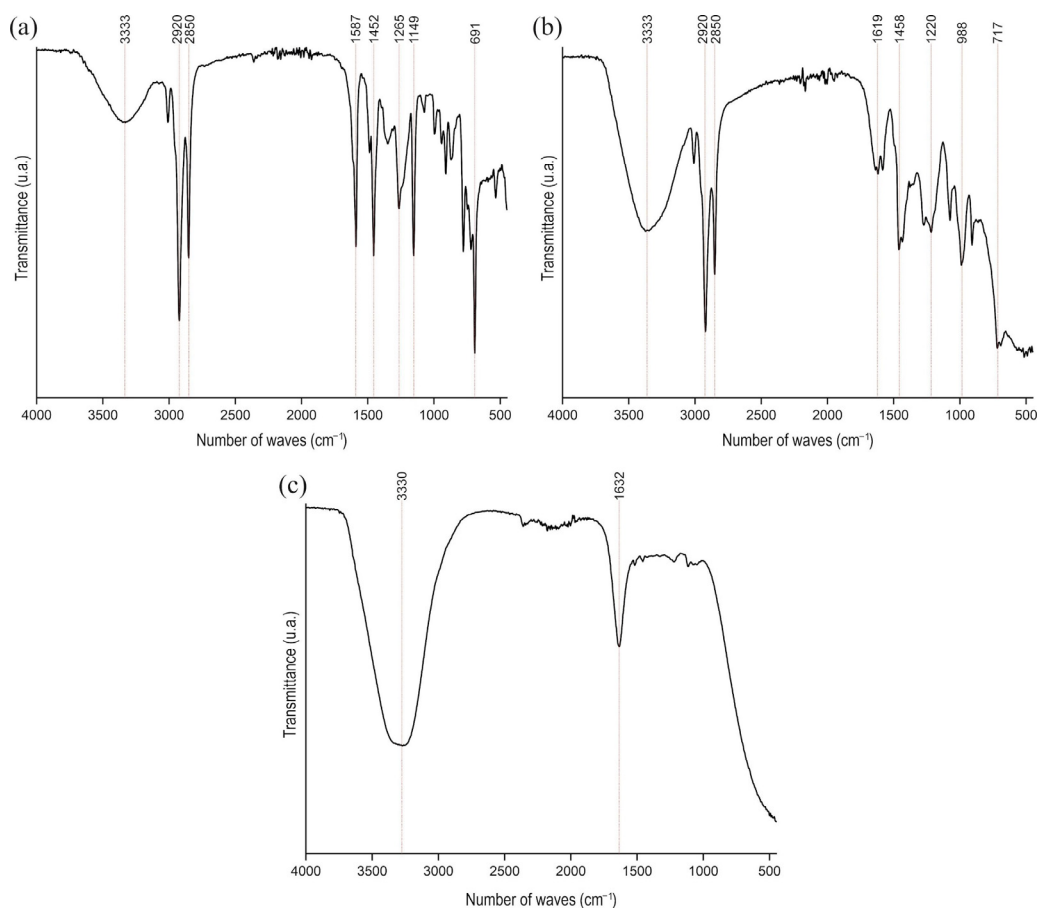
Figure 3. FTIR spectra with significant variations between 500 and 4000 cm^{-1}: (**a**) cardanol; (**b**) cardanol-formaldehyde adhesive; and (**c**) nanolignin.

The absorption band at 3333 cm^{-1} typically corresponds to O–H (hydroxyl) chemical bonds, which are present both in the phenolic structure of cardanol and in the guaiacyl and syringyl aromatic rings of lignin. This band was more prominent in the nanolignins at 3330 cm^{-1} (Figure 3c), indicating that the production of lignin nanoparticles using the top-down approach promoted greater reactivity, forming a higher number of hydrogen bonds [62].

The characteristic absorption bands at 2920 and 2850 cm^{-1} are related to the C–H stretching vibration of the aliphatic side chain present in cardanol. The peaks around 1592–1632 cm^{-1} indicate the presence of C=C bonds in the aromatic ring, while the peaks around 1452–1458 cm^{-1} correspond to C–H deformation vibration [63].

The peaks around 1220–1265 cm^{-1} correspond to C–O stretching vibrations in phenol, while the peaks around 1149 cm^{-1} are attributed to C–C skeletal vibrations. The bands around 988 cm^{-1} indicate C–H bonds in aromatic rings, whereas the peaks near 691 and 717 cm^{-1} suggest the presence of aliphatic chains. Similar results have been reported in Faria et al. [14], Balaji et al. [16] and Mestry et al. [63].

3.2. Adhesive Characterization

The viscosity of the cardanol-formaldehyde adhesives with nanolignin was lower than the control and did not differ statistically between 2 and 3% nanolignin (Table 2). Similar results were found by Faria et al. [14] with 1.55 Pa·s and by Furtini et al. [20], who found viscosity ranging from 1.81 to 0.11 Pa·s for urea-formaldehyde adhesive with cardanol in the composition. The high viscosity of adhesives (>1.5 Pa·s) tends to decrease their fluidity, which may result in low operability due to the difficulty of applying the adhesive. On the other hand, very low viscosity may result in exacerbated absorption by the panel, called a "hungry glue line", and impair the final product quality [55].

Table 2. Characterization of the cardanol-formaldehyde adhesive with different proportions of nanolignin.

| Treatment (Nanolignin Content %)	Viscosity (Pa·s)	Solids Content (%)	pH
0	2.32 ± 0.50 * c	95.82 ± 0.64 d	9.73 ± 0.07 c
1	1.49 ± 0.10 b	81.30 ± 0.69 c	9.57 ± 0.05 b
2	1.11 ± 0.10 a	75.23 ± 2.40 b	9.51 ± 0.10 b
3	0.74 ± 0.45 a	71.05 ± 0.18 a	9.39 ± 0.08 a

* Standard deviation; averages followed by the same letter in the same column do not differ significantly from each other by the Scott–Knott test at the 95% probability level.

The solids content showed statistical differences, contributing to the reduction in values as different proportions of nanolignin were added. According to Galdino et al. [64], the solids content indicates the percentage of reactive sites with the binder, with higher values resulting in more consistent and viscous adhesives. Faria et al. [14] found a solid content of 73.57% for the cardanol-formaldehyde adhesive, close to the treatments with 2 and 3% nanolignin. In the study carried out by Furtini et al. [20], as the cardanol concentrations increased, the solids content varied from 70.04 to 86.93%, while Parameswaran et al. [65] observed a solids content of 78% for the phenol-cardanol-formaldehyde adhesive and 81% for cardanol-formaldehyde, values close to this study.

The pH of the treatments with 1 and 2% nanolignin were statistically equal, and different from the control and 3% nanolignin. Furtini et al. [20] found pH ranging from 6.86 to 5.86, results lower than this study. Adhesives with relatively low pH can contribute to the degradation of lignocellulosic materials, while adhesives with high pH can provide foam in the glue line [14]. Nevertheless, the pH values of the present study did not impair the plywood production. These reductions in the solids content and pH values when adding nanolignin may be associated with the differences in crosslinking these adhesives [64]. Evaporation of unreacted formaldehyde may have occurred for resins with lower solids content and the water formed in the reaction since nanolignin suspension contains more than 90% water. Solt et al. [66] reported that resins with Kraft lignin have a longer gel time due to a lower value of free formaldehyde, compared to synthetic polymers.

Thermogravimetric analysis (Figure 4) presents the degradation process of the adhesives. The first stage occurred from 25 °C to approximately 100 °C, when all the adhesives lost mass due to the evaporation of water and other low-molecular-weight chemical compounds (e.g., formaldehyde) [67].
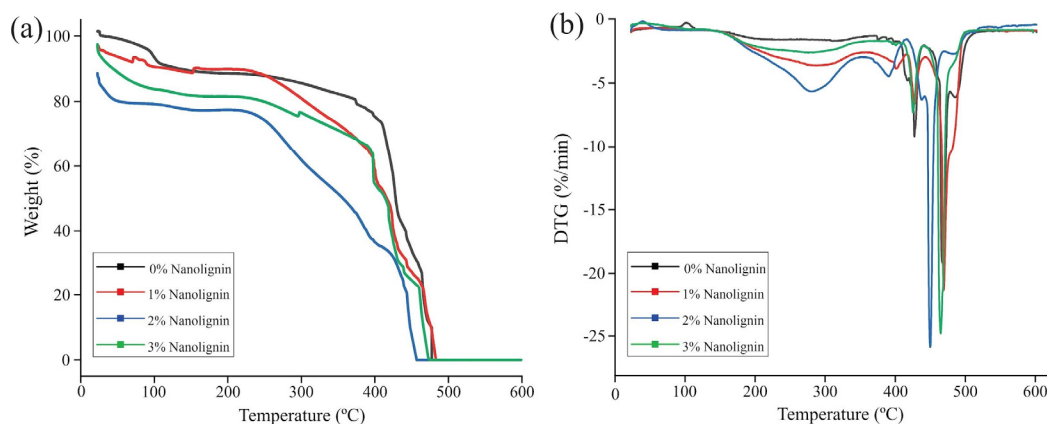
Figure 4. Thermal degradation of the adhesive. (**a**) Mass loss with increasing temperature; (**b**) first derivative of TGA (DTG).

Between 100 and 280 °C, all treatments show similar and apparently more stable decomposition performance. However, adhesives containing nanolignin progressively lose mass (4–18%) within this temperature range (Figure 4a). Nanolignin degrades at temperatures between 280 and 500 °C, with the greatest weight loss observed in the treatment containing 2% nanolignin. Between 400 and 500 °C, the mass loss of the adhesives was faster. This significant loss is attributed to the thermal decomposition of the phenolic/aromatic polymeric structure of lignin [68]. After approximately 500 °C, all adhesives are relatively stable up to around 600 °C.

The DTG curves indicate the temperature when the degradation rate was the maximum (Figure 4b). The highest peaks appear between 400 and 500 °C for all the samples. The pyrolytic degradation in this region for the adhesives with lignin nanostructures involves the fragmentation of bonds between lignin units, releasing monomeric phenols into the vapor phase. Only after 500 °C did all adhesives show highlighted similarities, with condensation reactions and the decomposition of aromatic rings in the lignin structures also occurring [22].

3.3. Physical–Mechanical and Microstructural Properties of Plywood

The average apparent density of the panels ranged from 0.75 to 0.79 g/cm^3, with no statistical difference between the treatments (Figure 5a). The apparent density of plywood depends on the wood species, the moisture content of the veneers, the temperature, and the pressing pressure used in manufacturing.

For moisture in the dry base of the plywood, there was no significant effect of any treatments (Figure 5b). The values were lower than those found in Pipíška et al. [69], when evaluating the moisture of plywood from *Picea abies* wood glued with phenol-urea-formaldehyde, under different pressures in adjacent layers, obtaining values ranging from 8.1 to 8.7% moisture. This result of the present study may indicate that the acclimatization period of the plywood before the tests was suitable, homogenizing their moisture contents.

The average water absorption after 2 and 24 h did not show statistical differences between treatments (Figure 6). This was probably due to cardanol, which presents hydrophobic characteristics, providing reduced water absorption [70]. In addition, the high specific surface area and porous structure of nanolignin may also contribute to increased

contact with the cardanol-formaldehyde adhesive, resulting in improved nanolignin reactivity and maintaining low water absorption of the plywood.
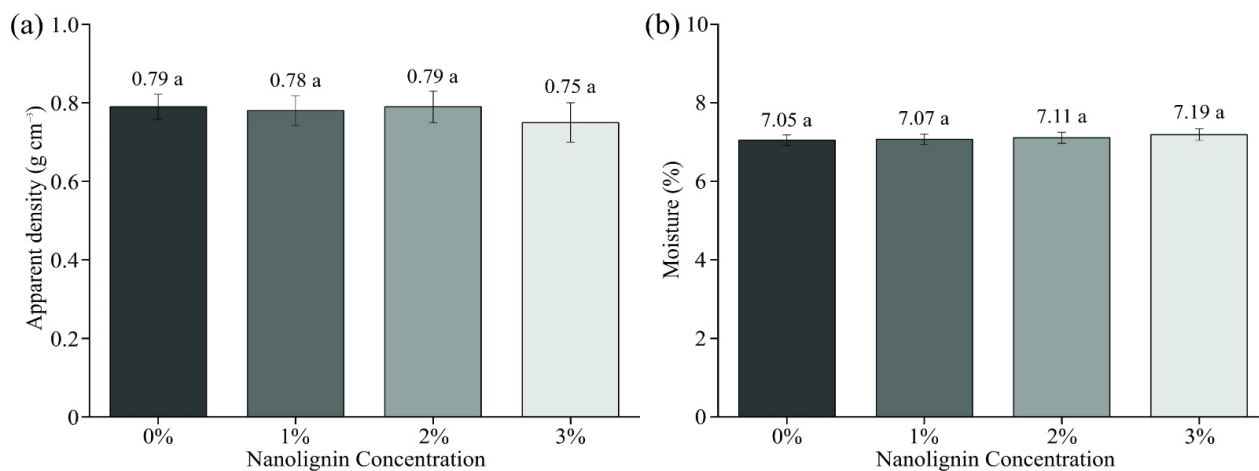
Figure 5. (**a**) Apparent density and (**b**) moisture content of plywood; averages followed by the same letter do not differ significantly by the Scott–Knott test at the 95% probability level.
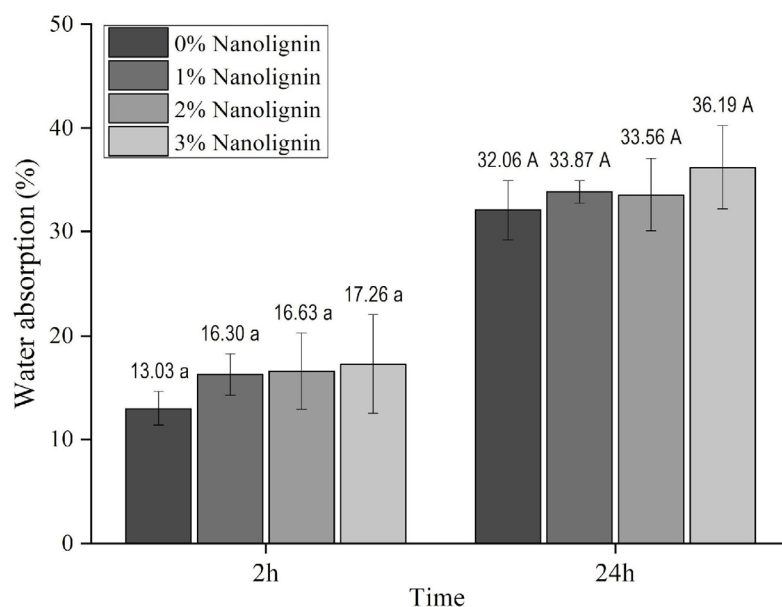

Figure 6. Water absorption after 2 and 24 h as a function of nanolignin concentration to the cardanol-formaldehyde adhesive; averages followed by the same letter do not differ significantly by the Scott–Knott test at the 95% probability level.

The present study obtained lower water absorption than that found by Setter et al. [71] working with *Schizolobium amazonicum* and *Pinus oocarpa* plywood glued with urea-formaldehyde (UF) and phenol-formaldehyde (PF), finding 82.84 and 67.36% with UF, and 71.93% and 62.76% with PF, respectively, of total water absorption in 24 h. Matos et al. [53] found 69.75% water absorption in *Pinus oocarpa* panels glued with PF. In the study by Younesi-Kordkheili et al. [72], nanolignin was used as a raw material to replace phenol, and combined with glyoxal, partially obtaining a reduction in water absorption. The same authors report that it may also be attributed to the difference in the number of bonds formed between the reactive sites. A different situation occurred in the study by Kordkheili et al. [73], in which phenol was replaced by modified lignin in phenol-formaldehyde resins, increasing the water absorption of the plywood. The authors explain that this may be related to the difference in the bonds formed in the lignin-phenol-formaldehyde adhesives

during the synthesis and due to the presence of absorbent sulfonic acid groups that are very sensitive to water in the lignin.

The shear strength in the glue line was influenced by the concentration of nanolignin (Figure 7). The boards glued only with cardanol-formaldehyde had the lowest shear strength value and differed statistically from the other treatments.
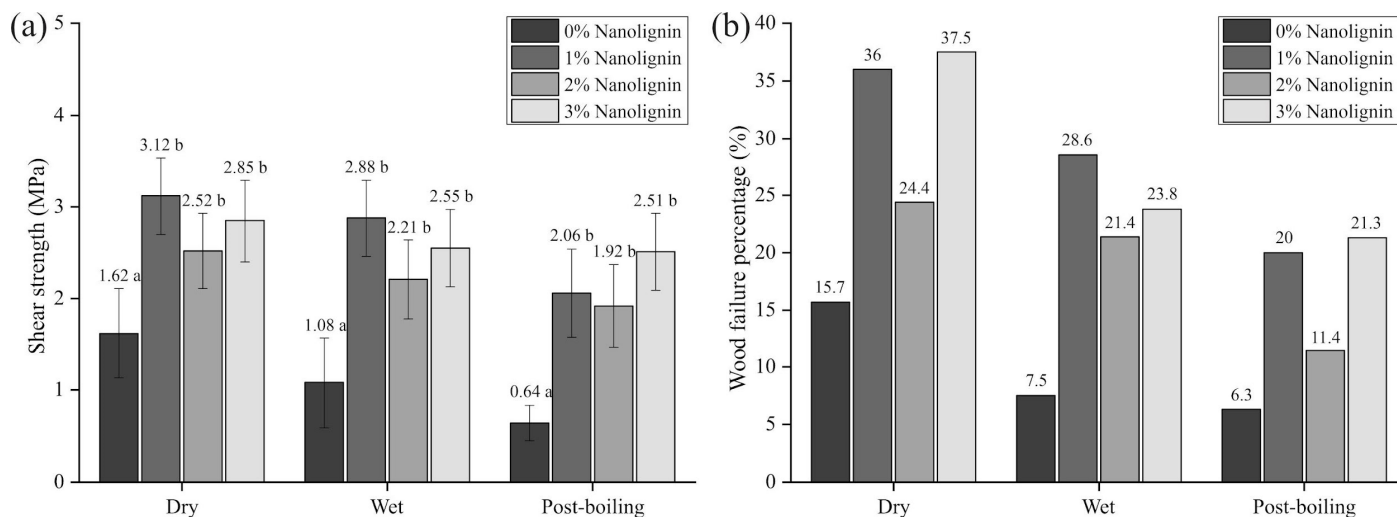

Figure 7. (**a**) Shear strength test results and (**b**) percentage of failure in dry, wet and post-boil conditions; averages followed by the same letter do not differ significantly from each other by the Scott–Knott test at the 95% probability level.

The values of this study were similar to those of Kordkheili et al. [74], increasing the percentage of phenol replacement by lignin from 10 to 20% by weight; the dry strength of the adhesives was increased from 2 to 2.4 MPa, while only the phenol-formaldehyde adhesive presented 1.7 MPa. In the study by Lengowski et al. [75], when nanocellulose was added to the phenol-formaldehyde adhesive, similar values for shear strength were obtained in dry tests. The first glue line varied from 1.09 MPa (with 0.064% nanocellulose) to 1.95 MPa (with 0.038% nanocellulose). The second glue line varied between 1.32 MPa (with phenol-formaldehyde adhesive) and 2.45 MPa (with 0.038% nanocellulose). Adhesives modified with nanostructures generally have more binding sites on their surface. Therefore, the surface properties can overlap the material's properties in its standard size, improving the mechanical properties of these adhesives.

In wet shear, Feng et al. [76] used *Betula alleghaniensis* three-layer plywood with phenol formaldehyde adhesive, exhibiting a wet bond strength of 2.09 MPa. The results of the present work were superior to those found by the same authors when they studied phenol-formaldehyde adhesives with an aqueous lignin solution in a weight ratio of 25/75 and found reduced wet bond strengths of 1.74 MPa. In addition, for the phenol-formaldehyde adhesive with methylated lignin solution (50/50), the wet shear strength was 1.43 MPa. In post-boiling shear (boiling for 6 h), Lengowski et al. [75] found average values ranging from 0.58 MPa (with 0.064% nanocellulose) to 0.75 MPa (phenol-formaldehyde adhesive) for the first glue line, and between 1.20 MPa (phenol-formaldehyde adhesive) and 1.55 MPa (with 0.064% nanocellulose) for the second glue line. Nanofibrillated cellulose improved the interaction of the adhesive with the wood, presenting greater resistance compared to the control sample. However, the boards met the requirements of EN—European Committee for Standardization [77], which specifies a minimum value of 1.0 MPa for tests under wood failure conditions, except for the post-boiling treatment without nanolignin concentration. Furthermore, the cardanol-formaldehyde adhesive with nanolignin has

a primary characteristic of high moisture resistance and can be indicated for indoor and outdoor use.

Figure 8 shows the results obtained from the static bending test in the parallel and perpendicular fiber directions.
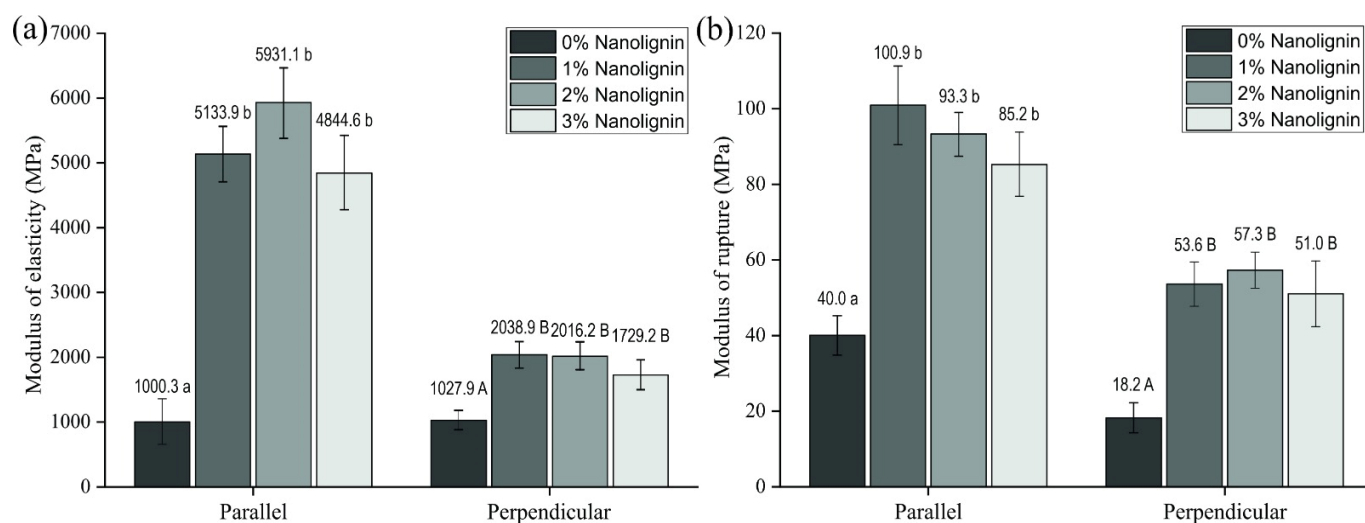
Figure 8. (**a**) Modulus of elasticity and (**b**) rupture with static bending in the parallel and perpendicular direction of the grain; averages followed by the same letter do not differ significantly by the Scott–Knott test at the 95% probability level.

In the modulus of elasticity in the parallel direction (Figure 8a), only the treatment with 2% nanolignin in the cardanol-formaldehyde adhesive met the requirements of the NBR 9531 [78] standard for plywood. In the perpendicular direction, all treatments with the addition of nanolignin were by the requirements. The standard establishes a minimum value of 5223 and 1485 MPa in parallel and perpendicular directions for external structural use.

In the modulus of rupture, the treatments with nanolignin in the cardanol-formaldehyde adhesive increased the rupture resistance in the parallel and perpendicular directions (Figure 8b). All treatments were by the NBR 9531 [78] standard, which allows the minimum required 30.9 MPa for parallel MOR and 14.0 MPa for perpendicular MOR. Reis et al. [79] analyzed *Pinus oocarpa* plywood glued with phenol-formaldehyde grammage of 320 g/m^2, with the same number of veneers, and found lower MOR values compared to the nanolignin treatments in the present study, with parallel MOR of 56.8 MPa and perpendicular of 31.5 MPa. They obtained similar results with parallel MOE of 4912 MPa and perpendicular MOE of 1808 MPa. Bilik et al. [80] found similar values to those previously mentioned when compared to the nanolignin treatments. They evaluated plywood panels glued with phenol-formaldehyde formulated with the addition of wheat flour and coconut shell, with parallel MOR of 45.36 MPa and perpendicular MOR of 32.05 MPa, while parallel MOE was 5139.78 MPa and perpendicular MOE 2590.96 MPa.

When analyzing plywood bonded with lignin-phenol-formaldehyde adhesives, Magalhães et al. [81] obtained parallel MOR of 10.29 MPa and perpendicular MOE of 38.42 MPa, as well as parallel MOE of 232.42 MPa and perpendicular MOE of 1804.41 MPa. These results diverge from the present study, where the addition of nanoscale lignin in the phenol-formaldehyde adhesive formulation improved mechanical properties.

SEM was used to observe the fractured surfaces of the plywood after the bending test. The micrographs show that the adhesive distribution on the particle surfaces was not uniform (Figure 9a,c). However, the wood veneers exhibited a complex porous structure, with the adhesive penetrating the pores to some extent, enabling mechanical interlocking,

as shown in Figure 9b,d. In particular, the tracheids in the wood veneer appear to have been partially filled with cardanol-formaldehyde adhesive with nanolignin. This penetration facilitated mechanical interlocking, thereby enhancing the mechanical properties.
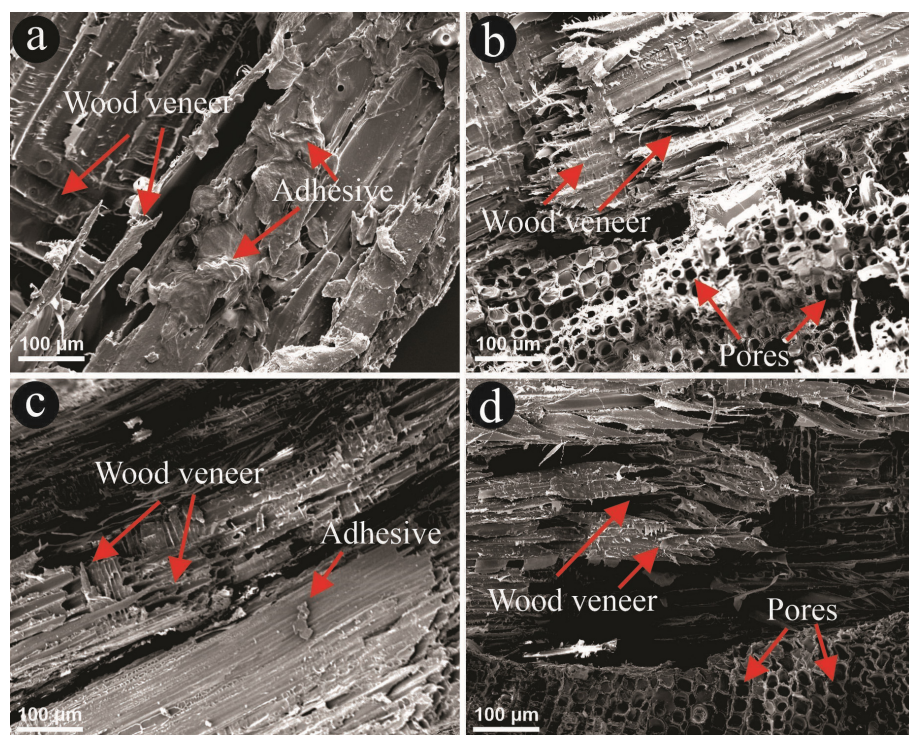

Figure 9. SEM micrographs of the fractured surface of plywood: (**a**) 0% nanolignin; (**b**) 1% nanolignin; (**c**) 2% nanolignin; (**d**) 3% nanolignin.

3.4. Thermal Properties of Plywood

In the combustion test of the plywood, the results are shown as a mass variation according to time (Figure 10). The panels produced with different proportions of nanolignin were more resistant to combustion (Figure 10a). This can be explained by the higher thermal resistance of lignin compared with the carbohydrates of wood (cellulose and hemicelluloses). Thus, its thermal degradation is between 225 °C and 450 °C, with exothermic reactions. At around 200 °C, dehydration reactions occur. Between 150 °C and 300 °C, the carbon bonds break, and, finally, at around 300 °C, the aliphatic lateral bonds begin to break outside the aromatic ring [14,82].

The temperature variations according to the combustion time (Figure 10b) show that the highest peak (450 °C) was obtained for the 1 and 2% nanolignin. The control treatment showed the lowest peak (415 °C). This peak appears after an initial heating when the volatile combustion gases are in sufficient quantity to allow ignition by an external spark igniter to support the ignition. The heat generated by the combustion sustains the thermal degradation process of the wood, thus releasing more volatiles. Therefore, the nanolignin may have influenced the reduction in the plywood degradation since the higher the combustion temperature in the first minutes, the faster the degradation of the cell wall [14,83]. The thermogravimetric analysis of the adhesives revealed greater thermal degradation of the cardanol-formaldehyde with nanolignin (see Figure 4). However, the additive may have acted as a combustion retardant in the plywood, contributing to lower thermal degradation of the composite material.
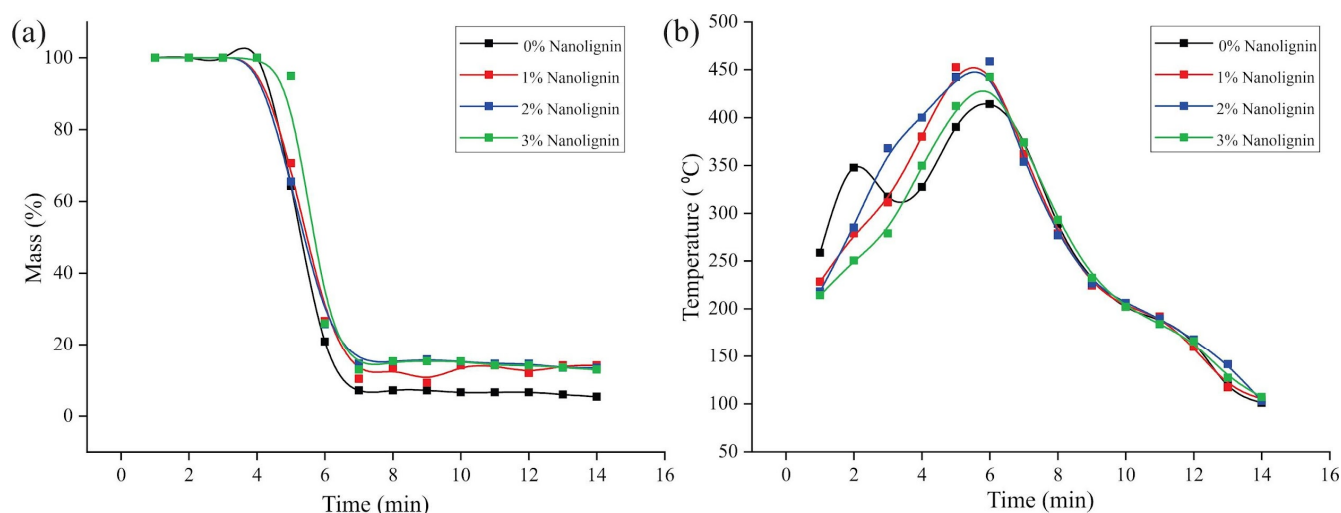
Figure 10. (**a**) Relationship between mass and combustion time; (**b**) temperature variation of plywood produced with cardanol-formaldehyde modified nanolignin.

The wood chemical characteristics mainly influence the panel combustibility. Up to 200 °C, the degradation of low-molar-mass compounds, such as extractives (greases, fatty acids, phenols, terpenes, steroids, acid resins, resins, and waxes), occurs first. Between 200 and 315 °C, hemicelluloses are degraded, cellulose between 300 and 400 °C, and then lignin between 300 and 600 °C [84–86].

In studies with cardanol-formaldehyde adhesive, Furtini et al. [20] observed that increases of up to 60% in cardanol efficiently delayed the combustion of the panels due to the chemical composition of cardanol, mainly due to the presence of the aromatic ring and the position of the double bonds, thus requiring more energy for thermal degradation. Similar results were found in Faria et al. [14], who observed that although the cardanol-formaldehyde adhesive was more resistant to combustion, adding bean residue reduced the thermal stability of the particleboard. This reduction was attributed to the chemical composition of the bean residue, which contained more extractives and less lignin.

Because of the results obtained, plywood glued with cardanol-formaldehyde modified with nanolignin may be attractive in the furniture and construction sectors. These panels may also contribute to reducing their combustibility or delaying combustion, thus demonstrating the benefits of these materials focused on environmental and security issues.

3.5. Formaldehyde Emission

The treatments presented statistical differences regarding free formaldehyde emission (Figure 11). When nanolignin was added to cardanol-formaldehyde, formaldehyde emission increased by 30.63, 72.63, and 85.76%, respectively, compared to the control.

Several researchers have indicated that the addition of nanolignin can effectively control formaldehyde emissions from wood-based panels [87–89]. However, in the present study, cardanol hindered free formaldehyde by reacting with the active sites of nanolignin after the synthesis, resulting in higher formaldehyde emissions. In adhesive production, the reaction between formaldehyde and nanolignin may have occurred only partially, and some unreacted formaldehyde may have led to higher emissions [7]. Despite the increase in formaldehyde emissions, all treatments comply with the standard EN 13986 [90], which establishes a value ≤ 80 mg/kg (class E1) for wood-based panels for construction. Faria et al. [14] reported an emission of 10.9 mg/kg for particleboard using cardanol-formaldehyde adhesive, higher than the value found in the present study.
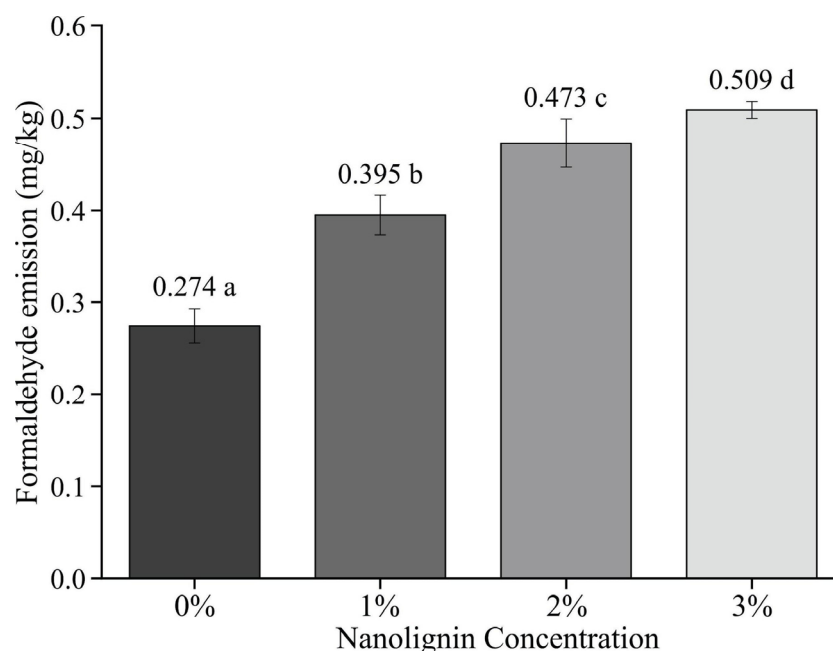
Figure 11. Free formaldehyde emission from plywood bonded with cardanol adhesive with nano-lignin; averages followed by the same letter do not differ significantly by the Scott–Knott test at the 95% probability level.

Taghiyari et al. [91] investigated the formaldehyde emissions in three-layer plywood produced with urea-formaldehyde adhesive with substitutions of 5, 10, 15, and 20% of soybean flour in the UF adhesive. The lowest emission value was 88.6 mg/kg for 20% substitution. On the other hand, Kawalerczyk et al. [92], when studying birch plywood, observed a slight reduction in formaldehyde emissions for 5% of cellulosic particles added to 100 g of solid UF, reaching 2 mg/kg. The methylene bonds (CH_2) that fully or partially surround the phenolic fractions are responsible for reducing formaldehyde emissions from the samples. Cardanol-formaldehyde as adhesive has potential in the wood-based panel industry. In addition to complying with structural standards regarding physical–mechanical properties, it also reduces formaldehyde emissions, which is the primary health benefit for the consumer [14].

The life cycle of cardanol as an adhesive for panels is marked by environmental benefits, especially when compared to conventional adhesives. It can offer renewable and biodegradable alternatives aligned with sustainability trends in the materials industry. The process of cashew cultivation can be optimized from the initial to the final use of the product to reduce environmental impacts. Nonetheless, there are still challenges in terms of recycling and disposal at the end of the useful life of the reconstituted panels. Modification with nanolignin and cardanol can result in a stronger and more flexible material with greater resistance to adverse environmental conditions. Cardanol can act as an agent that improves the chemical properties of nanolignin, while nanolignin can provide the necessary structure to create lighter and more environmentally friendly materials.

4. Conclusions

This study developed a cardanol-based adhesive enhanced with nanolignin, with the goal of improving plywood bonding and potentially reducing formaldehyde emissions. The combination of cardanol and nanolignin, both natural compounds, was explored as a sustainable alternative with lower environmental impact for use in the wood panel adhesive industry.

Due to the adhesive characteristics and the larger surface area of nanolignin, the technological properties of the plywood were affected. The plywood showed better values of shear at the glue line compared to the control (0% nanolignin) (e.g., 1.45 MPa for 2% nanolignin versus 1.18 MPa in the control), MOR (38.2 MPa versus 32.6 MPa) and MOE (5100 MPa versus 4400 MPa), with greater resistance to combustion. Despite the increase in formaldehyde emissions with nanolignin (from 0.274 mg/kg to 0.509 mg/kg), all treatments met the commercialization requirements ($\leq$80 mg formaldehyde/kg), demonstrating the adhesive potential for use in indoor environments. Thus, mechanical tests showed variations in strength parameters, indicating that this improvement strongly depends on the nanolignin concentration used. Therefore, the combination of cardanol and nanolignin in plywood offers a promising alternative for the production of more environmentally friendly and higher-performance construction materials, meeting the demand for more sustainable solutions in the wood industry.

For future research, it is recommended to develop more comprehensive characterization techniques for nanolignin and investigate the application of other agents or methods for the functionalization of the nanostructure. Furthermore, exploring different lignin sources with varying concentrations and different modification techniques for nanostructures can improve compatibility and achieve the desired effects on the final performance of the adhesive. Since in this study the nanolignin was not chemically modified, this may have resulted in agglomeration or poor interaction with the adhesive matrix. Furthermore, a limitation of this study was the high moisture during nanolignin dispersion, which may have contributed to the reduction in solids content and increased formaldehyde release. Therefore, it is recommended to conduct future studies exploring the use of modified nanolignin, more efficient drying techniques, and a more in-depth characterization of nanolignin dispersion in the adhesive matrix.

Author Contributions: Writing—Original Draft and Project Administration, M.R.R.M. and F.G.B.; Methodology, Conceptualization and Investigation, A.C.C.F. and F.M.S.B.; Formal Analysis, Writing—review and editing, M.V.S. and T.d.P.P.; Supervision, Funding Acquisition and Resources, L.M.M. and J.B.G.J. All authors have read and agreed to the published version of the manuscript.

Data Availability Statement: Derived data supporting the findings of this study are available from the corresponding author upon request.

Conflicts of Interest: The authors declare no conflicts of interest.

References

1. Zeng, G.; Zhou, Y.; Liang, Y.; Zhang, F.; Luo, J.; Li, J.; Fang, Z. A hair fiber inspired bio-based adhesive with high bonding strength and mildew tolerance. *Chem. Eng. J.* **2022**, *434*, 134632. [CrossRef]
2. Mili, M.; Hashmi, S.A.R.; Ather, M.; Hada, V.; Markandeya, N.; Kamble, S.; Mohapatra, M.; Rathore, S.K.S.; Srivastava, A.K.; Verma, S. Novel lignin as natural-biodegradable binder for various sectors—A review. *J. Appl. Polym. Sci.* **2022**, *139*, 51951. [CrossRef]
3. Oktay, S.; Kızılcan, N.; Bengü, B. Environment-friendly cornstarch and tannin-based wood adhesives for interior particleboard production as an alternative to formaldehyde-based wood adhesives. *Pigment Resin Technol.* **2024**, *53*, 173–182. [CrossRef]

4. Selakjani, P.P.; Dorieh, A.; Pizzi, A.; Shahavi, M.H.; Hasankhah, A.; Shekarsaraee, S.; Ashouri, M.; Movahed, S.G.; Abatari, M.N. Reducing free formaldehyde emission, improvement of thickness swelling and increasing storage stability of novel medium density fiberboard by urea-formaldehyde adhesive modified by phenol derivatives. *Int. J. Adhes. Adhes.* **2021**, *111*, 102962. [CrossRef]

5. Khanjanzadeh, H.; Behrooz, R.; Bahramifar, N.; Pinkl, S.; Gindl-Altmutter, W. Application of surface chemical functionalized cellulose nanocrystals to improve the performance of UF adhesives used in wood-based composites-MDF type. *Carbohydr. Polym.* **2019**, *206*, 11–20. [CrossRef]

6. Raydan, N.D.V.; Leroyer, L.; Charrier, B.; Robles, E. Recent advances on the development of protein-based adhesives for wood composite materials—A review. *Molecules* **2021**, *26*, 7617. [CrossRef] [PubMed]

7. Chen, Y.; Gong, X.; Yang, G.; Li, Q.; Zhou, N. Preparation and characterization of a nanolignin phenol formaldehyde resin by replacing phenol partially with lignin nanoparticles. *RSC Adv.* **2019**, *9*, 29255–29262. [CrossRef]

8. Wang, P.; Liu, J.; Chi, C.; Zhang, Y.; Chen, D.; Chen, Q. Solvent-free synthesis, plasticization and compatibilization of cardanol grafted onto liquid isoprene rubber. *Compos. Sci. Technol.* **2021**, *215*, 109027. [CrossRef]

9. Wang, H.; Zhang, C.; Zeng, W.; Zhou, Q. Making alkyd greener: Modified cardanol as bio-based reactive diluents for alkyd coating. *Prog. Org. Coat.* **2019**, *135*, 281–290. [CrossRef]

10. Bo, C.; Shi, Z.; Hu, L.; Pan, Z.; Hu, Y.; Yang, X.; Zhang, M.; Zhou, Y. Cardanol derived P, Si and N based precursors to develop flame retardant phenolic foam. *Sci. Rep.* **2020**, *10*, 12082. [CrossRef]

11. Jadhav, N.L.; Sastry, S.K.C.; Pinjari, D.V. Energy efficient room temperature synthesis of cardanol-based novolac resin using acoustic cavitation. *Ultrason. Sonochem.* **2018**, *42*, 532–540. [CrossRef] [PubMed]

12. Moita Neto, J.M.; Lopes, J.A.D.; Lima, S.G.; Macedo, A.O.A.; Citó, A.M.G.L. Resina tipo resol do líquido da casca da castanha de caju. *An. ABQ* **1997**, *46*, 220–223.

13. França, F.C.; Coelho, E.D.L.; Uchôa, A.F.; Rodrigues, F.H.; Ribeiro, M.E.; Soares, S.D.A.; Ricardo, N.M. Synthesis and characterization of alkylphenyl polyglycosidic surfactants from amylose and alkyl phenols extracted from natural CNSL. *Química Nova* **2016**, *39*, 771–781. [CrossRef]

14. Faria, D.L.; Scatolino, M.V.; Oliveira, J.E.; Gonçalves, F.G.; Soriano, J.; Paula Protásio, T.; Junior, J.B.G. Cardanol-based adhesive with reduced formaldehyde emission to produce particleboards with waste from bean crops. *Environ. Sci. Pollut. Res.* **2023**, *30*, 48270–48287. [CrossRef] [PubMed]

15. Santos, R.S.; Souza, A.A.; Paoli, M.; Souza, C.M.L. Cardanol–formaldehyde thermoset composites reinforced with buriti fibers: Preparation and characterization. *Compos Part A Appl. Sci.* **2010**, *41*, 1123–1129. [CrossRef]

16. Balaji, A.; Karthikeyan, B.; Swaminathan, J.; Raj, C.S. Mechanical behavior of short bagasse fiber reinforced cardanol-formaldehyde composites. *Fibers Polym.* **2017**, *18*, 1193–1199. [CrossRef]

17. Balaji, A.; Karthikeyan, B.; Swaminathan, J.; Raj, C.S. Effect of filler content of chemically treated short bagasse fiber-reinforced cardanol polymer composites. *J. Nat. Fibers* **2019**, *16*, 613–627. [CrossRef]

18. Shislov, O.F.; Troshin, D.P.; Baulina, N.S.; Glukhikh, V.V.; Stoyanov, O.V. Synthesis and properties of glues for densified laminated wood based on alcohol-soluble phenol–cardanol–formaldehyde resolic resins. *Polym Sci.* **2015**, *8*, 37–41. [CrossRef]

19. Caillol, S. Cardanol: A promising building block for biobased polymers and additives. *Curr. Opin. Green Sustain. Chem.* **2018**, *14*, 26–32. [CrossRef]

20. Furtini, A.C.C.; Brito, F.M.S.; Junior, M.G.; Furtini, J.A.O.; Pinto, L.M.A.; Protásio, T.P.; Mendes, L.M.; Guimarães, J.B., Jr. Substitution of urea–formaldehyde by renewable phenolic compound for environmentally appropriate production of particleboards. *Environ. Sci. Pollut. Res.* **2022**, *29*, 66562–66577. [CrossRef]

21. Torres, L.A.Z.; Woiciechowski, A.L.; Andrade Tanobe, V.O.; Karp, S.G.; Lorenci, L.C.G.; Faulds, C.; Soccol, C.R. Lignin as a potential source of high-added value compounds: A review. *J. Clean. Prod.* **2020**, *263*, 121499. [CrossRef]

22. Gendron, J.; Stambouli, I.; Bruel, C.; Boumghar, Y.; Montplaisir, D. Characterization of different types of lignin and their potential use in green adhesives. *Ind. Crops Prod.* **2022**, *182*, 114893. [CrossRef]

23. Kalami, S.; Chen, N.; Borazjani, H.; Nejad, M. Comparative analysis of different lignins as phenol replacement in phenolic adhesive formulations. *Ind. Crops Prod.* **2018**, *125*, 520–528. [CrossRef]

24. Collins, M.N.; Nechifor, M.; Tanasă, F.; Zănoagă, M.; McLoughlin, A.; Stróżyk, M.A.; Culebras, M.C.-A. Teacă Valorization of lignin in polymer and composite systems for advanced engineering applications—A Review. *Int. J. Biol. Macromol.* **2019**, *131*, 828–849. [CrossRef]

25. Li, W.; Sun, H.; Wang, G.; Sui, W.; Dai, l.; Si, C. Lignin as a green and multifunctional alternative to phenol for resin synthesis. *Green Chem.* **2023**, *25*, 2241–2261. [CrossRef]

26. Gao, Z.; Lang, X.; Chen, S.; Zhao, C. Mini-review on the synthesis of lignin-based phenolic resin. *Energy Fuels* **2021**, *35*, 18385–18395. [CrossRef]

27. Bansode, A.; Barde, M.; Asafu-Adjaye, O.; Patil, V.; Hinkle, J.; Via, B.K.; Adhikari, S.; Adamczyk, A.J.; Farag, R.T. Elder Synthesis of biobased novolac phenol-formaldehyde wood adhesives from biorefinery-derived lignocellu-losic biomass. *ACS Sustain. Chem. Eng.* **2021**, *9*, 10990–11002. [CrossRef]

28. Zhou, J.; Hu, L.; Zhou, Y.; Jia, P.B. Liang Liquefaction and characterization of enzymatic hydrolysis lignin with phosphotungstic acid. *Cellul. Chem. Technol.* **2018**, *52*, 387–391.

29. Ren, X.; Lin, W.; Wang, Z.; Shi, Z.; Zheng, C. Liu Preparation of high molecular weight thermoplastic bio-based phenolic resin and fiber based on lignin liquefaction Mater. *Res. Express* **2021**, *8*, 015308. [CrossRef]

30. Liu, J.; Zhu, Y.; Gong, Z.; Chang, Z.; Meng, Y.; Qu, W.; Zhu, C. Prepara-tion and characterization of lignin copolymerized phenolic resins with superior stiff-ening effect for natural rubber composites. *Polymer* **2024**, *308*, 127366. [CrossRef]

31. Luckman, S.S.; Cunha, A.B.; Rios, P.D.; Zanatta, P. Influência da incorporação de lignina Kraft à resina ureia-formaldeído nas propriedades tecnológicas de painéis aglomerados convencionais. *Sci. For.* **2021**, *49*, e3527. [CrossRef]

32. Nair, S.S.; Sharma, S.; Pu, Y.; Sun, Q.; Pan, S.; Zhu, J.Y.; Deng, Y.; Ragauskas, A.J. High shear homogenization of lignin to nanolignin and thermal stability of Nanolignin-Polyvinyl alcohol blends. *ChemSusChem* **2014**, *7*, 3513–3520. [CrossRef] [PubMed]

33. Xue, Z.; Sun, H.; Wang, G.; Sui, W.; Jia, H.; Si, C. Fabrication modulation of lignin-derived carbon nanosphere supported Pd nanoparticle via lignin fraction-ation for improved catalytic performance in vanillin hydrodeoxygenation. *Int. J. Biol. Macromol.* **2024**, *258*, 128963. [CrossRef]

34. Gong, X.; Meng, Y.; Lu, J.; Tao, Y.; Cheng, Y.; Wang, H. A review on lignin-based phenolic resin adhesive. *Macromol. Chem. Phys.* **2022**, *223*, 2100434. [CrossRef]

35. Younesi-Kordkheili, H.; Pizzi, A.; Erfani, S.; Amiri, M. The synthesis of maleated nanolignin–polyvinyl alcohol–hexamine resin as a cold-setting wood adhesive. *Eur. J. Wood Wood Prod.* **2024**, *82*, 159–166. [CrossRef]

36. Zhu, Y.; Bian, R.; Yu, Y.; Li, J.; Li, C.; Lyu, Y.; Li, J. Aminated alkali lignin nanoparticles enabled formaldehyde-free biomass wood adhesive with high strength, toughness, and mildew resistance. *Chem. Eng. J.* **2024**, *494*, 152914. [CrossRef]

37. Lopes, T.A.; Lopes, N.F.; Portilho, G.R.; Andrade, F.A.; Silva, L.B.J.; Castro, R.V.O.; Tonoli, G.H.D.; Carneiro, A.D.C.O. Nano-Partículas de Lignina e Seus Efeitos nas Propriedades do Adesivo Ureia-Formaldeído para Colagem de Madeira. In *Engenharia Industrial Madeireira: Tecnologia, Pesquisa e Tendências*, 1st ed.; Gonçalves, F.G., Ed.; Editora Científica Digital: São Paulo, Brazil, 2020; pp. 219–242.

38. *NBR 11941*; Wood: Basic Density Efficiency. ABNT: Rio de Janeiro, Brazil, 2003.

39. *T 204 om-97*; Solvent Extractives of Wood and Pulp. TAPPI: Atlanta, GA, USA, 1997.

40. *T 222 om-02*; Acid-Insoluble Lignin in Wood Pulp. TAPPI: Atlanta, GA, USA, 2002.

41. *211 om-02*; Ash in Wood, Pulp, Paper and Paperboard: Combustion at 525 °C. TAPPI: Atlanta, GA, USA, 2002.

42. Browning, B.L. *The Chemistry of Wood*; J. Wiley: New York, NY, USA, 1963; p. 689.

43. *D 1490-01*; Standard Test Method for Nonvolatile Content of Urea-Formaldehyde Resin Solutions. ASTM International: West Conshohocken, PA, USA, 2013.

44. *D 1200-10*; Standard Test Method for Viscosity by Ford Viscosity Cup. ASTM International: West Conshohocken, PA, USA, 2010.

45. *ABNT NBR 9485*; Compensado: Determinação da Massa Específica Aparente. ABNT. Brazilian Association of Technical Standards: Rio de Janeiro, Brazil, 2011.

46. *ABNT NBR 9484*; Compensado: Determinação do Teor de Umidade. ABNT. Brazilian Association of Technical Standards: Rio de Janeiro, Brazil, 2011.

47. *ABNT NBR 9586*; Compensado—Determinação da Absorção de Água. ABNT. Brazilian Association of Technical Standards: Rio de Janeiro, Brazil, 2011.

48. *ABNT NBR ISO 12466-1*; Madeira Compensada: Qualidade de Colagem: Parte 1: Métodos de Ensaio. ABNT: Rio de Janeiro, Brazil, 2012.

49. *ABNT NBR 9533*; Compensado: Determinação da Resistência à Flexão estática. ABNT. Brazilian Association of Technical Standards: Rio de Janeiro, Brazil, 2012.

50. *EN 717-3*; Wood-Based Panels—Determination of Formaldehyde Release, Part 3: Formaldehyde Release by the Flask Method. 1996. Available online: https://www.en-standard.eu/bs-en-717-3-1996-wood-based-panels-determination-of-formaldehyde-release-formaldehyde-release-by-the-flask-method/?gclid=Cj0KCQiA1ZGcBhCoARIsAGQ0kkrFkuQ2YIEtzBkQ3TJxzZtTuRQQXrQNP3xumprDfnqr03LyoARtY_saAl2zEALw_wcB (accessed on 31 January 2025).

51. Setter, C.; Borges, F.A.; Cardoso, C.R.; Mendes, R.F.; Oliveira, T.J.P. Energy quality of pellets produced from coffee residue: Characterization of the products obtained via slow pyrolysis. *Ind. Crops Prod.* **2020**, *154*, 112731. [CrossRef]

52. Faria, D.L.; Gonçalves, F.G.; Maffioletti, F.D.; Scatolino, M.V.; Soriano, J.; Paula Protásio, T.; Lopez, Y.M.; Paes, J.B.; Mendes, L.M.; Guimarães Junior, J.B.; et al. Particleboards based on agricultural and agroforestry wastes glued with vegetal polyurethane adhesive: An efficient and eco-friendly alternative. *Ind. Crops Prod.* **2024**, *214*, 118540. [CrossRef]

53. Matos, A.C.; Guimarães Junior, J.B.; Borges, C.C.; Matos, L.C.; Ferreira, J.C.; Mendes, L.M. Influência de diferentes composições estruturais de *Schizolobium parahyba* var. *amazonicum* (Huber ex Ducke) Barneby e *Pinus oocarpa* var. *oocarpa* (Schiede ex Schltdl) para a produção de compensados multilaminados. *Sci. For.* **2019**, *124*, 799–810.

54. Brito, F.M.S.; Mendes, L.M.; Silva, P.X.S.; Júnior, J.B.G.; Palumbo, S.K.C. Technological characterization of particleboards constituted with pistachio shell (*Pistacia vera*) and *Pinus oocarpa* wood. *Rev. Bras. Ciências Agrárias* **2021**, *16*, e8902. [CrossRef]

55. Iwakiri, S.; Trianoski, R. *Painéis de Madeira Reconstituída*; Scientia Forestalis: Curitiba, Brazil, 2020; pp. 7–8.

56. Lourenço, Y.B.C.; Santos, C.A.D.; Furtini, A.C.C.; Mendes, L.M.; Guimarães Junior, J.B. Utilization of nanotalc modified adhesives in plywood panels. *Maderas. Cienc. Tecnol.* **2024**, *26*. [CrossRef]

57. Furtini, A.C.C.; Santos, C.A.D.; Garcia, H.V.S.; Brito, F.M.S.; Santos, T.P.D.; Mendes, L.M.; Guimarães Júnior, J.B. Performance of cross laminated timber panels made of *Pinus oocarpa* and *Coffea arabica* waste. *Coffee Sci.* **2021**, *16*, e161854. [CrossRef]

58. Santiago, S.B.; Gonçalves, F.G.; Lelis, R.C.C.; Segundinho, P.G.A.; Paes, J.B.; Arantes, M.D.C. Colagem de madeira de eucalipto com adesivos naturais. *Rev. Matéria* **2018**, *23*, e12151. [CrossRef]

59. Villarruel, D.C.V.; Novais Miranda, E.H.; Gomes, D.A.C.; Furtini, A.C.C.; Santos, C.A.; Mendes, L.M.; Guimarães Júnior, J.B. Evaluation of the addition of wheat residues in the production of *Pinus oocarpa* agglomerated panels. *Clean Technol. Environ. Policy* **2023**, *25*, 1753–1760. [CrossRef]

60. Sun, B.; Wang, Z.; Liu, J. Changes of chemical properties and the water vapour sorption of *Eucalyptus pellita* wood thermally modified in vacuum. *J. Wood Sci.* **2017**, *63*, 133–139. [CrossRef]

61. Neitzel, N.; Hosseinpourpia, R.; Walther, T.; Adamopoulos, S. Alternative materials from agro-industry for wood panel manufacturing—A review. *Materials* **2022**, *15*, 4542. [CrossRef]

62. Osterberg, M.; Sipponen, M.H.; Mattos, B.D.; Rojas, O.J. Spherical lignin particles: A review on their sustainability and applications. *Green Chem.* **2020**, *22*, 2712–2733. [CrossRef]

63. Mestry, S.U.; Khuntia, S.P.; Mhaske, S.T. Development of waterborne polyurethane dispersions (WPUDs) from novel cardanol-based reactive dispersing agent. *Polym. Bull.* **2021**, *78*, 6819–6834. [CrossRef]

64. Galdino, D.S.; Kondo, M.Y.; Araujo, V.A.; Ferrufino, G.L.A.A.; Faustino, E.; Santos, H.F.D.; Christoforo, A.L.; Luna, C.M.R.; Campos, C.I.D. Thermal and gluing properties of phenol-based resin with lignin for potential application in structural composites. *Polymers* **2023**, *15*, 357. [CrossRef]

65. Parameswaran, P.S.; Abraham, B.T.; Thachil, E.T. Cardanol-based resol phenolics—A comparative study. *Progress Rubber Plast. Recycl. Technol.* **2010**, *26*, 31–50. [CrossRef]

66. Solt, P.; Rößiger, B.; Konnerth, J.; Van Herwijnen, H.W. Lignin phenol formaldehyde resoles using base-catalysed depolymerized kraft lignin. *Polymers* **2018**, *10*, 1162. [CrossRef]

67. Papadopoulou, E.; Wild, P.J.; Kountouras, S.; Chrissafis, K. Evaluation of torrefaction condensates as phenol substitutes in the synthesis of phenol-formaldehyde adhesives suitable for plywood. *Thermochimica Acta* **2018**, *663*, 27–33. [CrossRef]

68. Pappa, C.P.; Cailotto, S.; Gigli, M.; Crestini, C.; Triantafyllidis, K.S. Kraft (Nano) Lignin as reactive additive in epoxy polymer bio-composites. *Polymers* **2024**, *16*, 553. [CrossRef] [PubMed]

69. Pipíška, T.; Bekhta, P.; Král, P.; Paschová, Z. Effects of different pressures and veneer moisture content in adjacent layers on properties of PUF bonded plywood. *J. Adhesion Sci. Technol.* **2024**, *38*, 1043–1052. [CrossRef]

70. Caillol, S. The future of cardanol as small giant for biobased aromatic polymers and additives. *Eur. Polym. J.* **2023**, *193*, 112096. [CrossRef]

71. Setter, C.; Zidanes, U.L.; Novais Miranda, E.H.; Brito, F.M.S.; Mendes, L.M.; Junior, J.B.G. Influence of wood species and adhesive type on the performance of multilaminated plywood. *Environ. Sci. Pollut. Res.* **2021**, *28*, 50835–50846. [CrossRef]

72. Younesi-Kordkheili, H.; Pizzi, A. Improving the properties of phenol-lignin-glyoxal as a wood adhesive by lignin nanoparticles. *Eur. J. Wood Wood Prod.* **2023**, *81*, 507–512. [CrossRef]

73. Kordkheili, H.Y.; Pizzi, A. Improving properties of phenol-lignin-glyoxal resin as a wood adhesive by an epoxy resin. *Eur. J. Wood Wood Prod.* **2021**, *79*, 199–205. [CrossRef]

74. Kordkheili, H.Y.; Pizzi, A. Properties of plywood panels bonded with ionic liquid-modified lignin–phenol–formaldehyde resin. *J. Adhesion* **2018**, *94*, 143–154. [CrossRef]

75. Lengowski, E.C.; Bonfatti Júnior, E.A.; Dallo, R.; Nisgoski, S.; Mattos, J.L.M.D.; Prata, J.G. Nanocellulose-reinforced phenol-formaldehyde resin for plywood panel production. *Maderas Cienc. Tecnol.* **2021**, *23*. [CrossRef]

76. Feng, S.; Shui, T.; Wang, H.; Ai, X.; Kuboki, T.; Xu, C.C. Properties of phenolic adhesives formulated with activated organosolv lignin derived from cornstalk. *Ind. Crops Prod.* **2021**, *161*, 113225. [CrossRef]

77. *EN 310*; Wood based panels – Determination of modulus of elasticity and modulus of rupture in static bending. EN—European Committee for Standardization: Brussels, Belgium, 1993.

78. *NBR 9531*; Plywood Sheets: Classification. ABNT: Rio de Janeiro, Brazil, 1986.

79. Reis, A.H.S.; Silva, D.W.; Vilela, A.P.; Mendes, R.F.; Mendes, L.M. Physical-mechanical properties of plywood produced with *Acrocarpus fraxinifolius* and *Pinus oocarpa*. *Floresta Ambiente* **2019**, *26*, e20170157. [CrossRef]

80. Bilik, A.C.B.; Trianoski, R. Evaluation of the physico-mechanical properties of plywood panels and laminated veneer lumber of *Pinus glabra* Walt. *Floresta* **2022**, *52*, 323–331. [CrossRef]

81. Magalhães, M.A.; Vital, B.R.; Carneiro, A.C.O.; Silva, C.M.D.; Fialho, L.F.; Figueiro, C.G.; Ferreira, J.C. Adição de lignina Kraft à resina fenólica para a fabricação de compensados. *Ciência Madeira* **2019**, *10*, 142–149. [CrossRef]

82. Sardar, N.M.; Rasim, Y.K. Fire retardant and fungi protection materials for wood constructions. *J. Pharm. Negat. Results* **2023**, 1023–1026. [CrossRef]

83. Sharma, R.K.; Wooten, J.B.; Baliga, V.L.; Lin, X.; Chan, W.G.; Hajaligol, M.R. Characterization of chars from pyrolysis of lignin. *Fuel* **2004**, *83*, 1469–1482. [CrossRef]

84. Bianchi, O.; Dal Castel, C.; Oliveira, R.V.B.; Bertuoli, P.T.; Hillig, E. Nonisothermal degradation of wood using thermogravimetric measurements. *Polímeros* **2010**, *20*, 395–400. [CrossRef]

85. Floch, A.; Jourdes, M.; Teissedre, P. Polysaccharides and lignin from oak wood used in cooperage: Composition, interest, assays: A review. *Carbohydr. Res.* **2015**, *417*, 94–102. [CrossRef]

86. Martínez, M.G.; Couce, A.A.; Dupont, C.; Silva Perez, D.; Thiéry, S.; Meyer, X.M.; Gourdon, C. Torrefaction of cellulose, hemicelluloses and lignin extracted from woody and agricultural biomass in TGA-GC/MS: Linking production profiles of volatile species to biomass type and macromolecular composition. *Ind. Crops Prod.* **2022**, *176*, 114350. [CrossRef]

87. Dorieh, A.; Pahlavan, F.; Hájková, K.; Hýsek, Š.; Farajollah Pour, M.; Fini, H. Advancing Sustainable Building Materials: Reducing Formaldehyde Emissions in Medium Density Fiber Boards with Lignin Nanoparticles. *Adv. Sustain. Syst.* **2024**, *8*, 2400102. [CrossRef]

88. Núñez-Decap, M.; Friz-Sánchez, C.; Opazo-Carlsson, C.; Moya-Rojas, B.; Vidal-Vega, M. A Potential Replacement to Phenol–Formaldehyde-Based Adhesives: A Study of Plywood Panels Manufactured with Bio-Based Wood Protein and Nanolignin Adhesives. *Forests* **2024**, *15*, 1345. [CrossRef]

89. Younesi-Kordkheili, H. Reduction of formaldehyde emission from urea-formaldehyde resin by maleated nanolignin. *Int. J. Adhes. Adhes.* **2024**, *132*, 103677. [CrossRef]

90. *BS EN 13986:2004+A1:2015*; Wood-Based Panels for Use in Construction. Characteristics, Evaluation of Conformity and Marking. BSI: London, UK, 2015. Available online: https://www.en-standard.eu/bs-en-13986-2004-a1-2015-wood-based-panels-for-use-in-construction-characteristics-evaluation-of-conformity-and-marking/?gclid=Cj0KCQiA1ZGcBhCoARIsAGQ0kkojpktyTiMbjpzkCuN-cqBxxnO06mf87HBrZ885l27F45WSQrOnbnAaAhTwEALw_wcB (accessed on 24 January 2025).

91. Taghiyari, H.R.; Hosseini, S.B.; Ghahri, S.; Ghofrani, M.; Papadopoulos, A.N. Formaldehyde emission in micron-sized wollastonite-treated plywood bonded with soy flour and urea-formaldehyde resin. *Appl. Sci.* **2020**, *10*, 6709. [CrossRef]

92. Kawalerczyk, J.; Dziurka, D.; Mirski, R.; Szentner, K. Properties of plywood produced with urea-formaldehyde adhesive modified with nanocellulose and microcellulose. *Drv. Ind.* **2020**, *71*, 61–67. [CrossRef]